Supplementary Information

Full control of ligand positioning reveals spatial thresholds for T cell receptor triggering

Haogang Cai, James Muller, David Depoil, Viveka Mayya, Michael P. Sheetz, Michael L. Dustin, and Shalom J. Wind

Nanoarray fabrication process flow

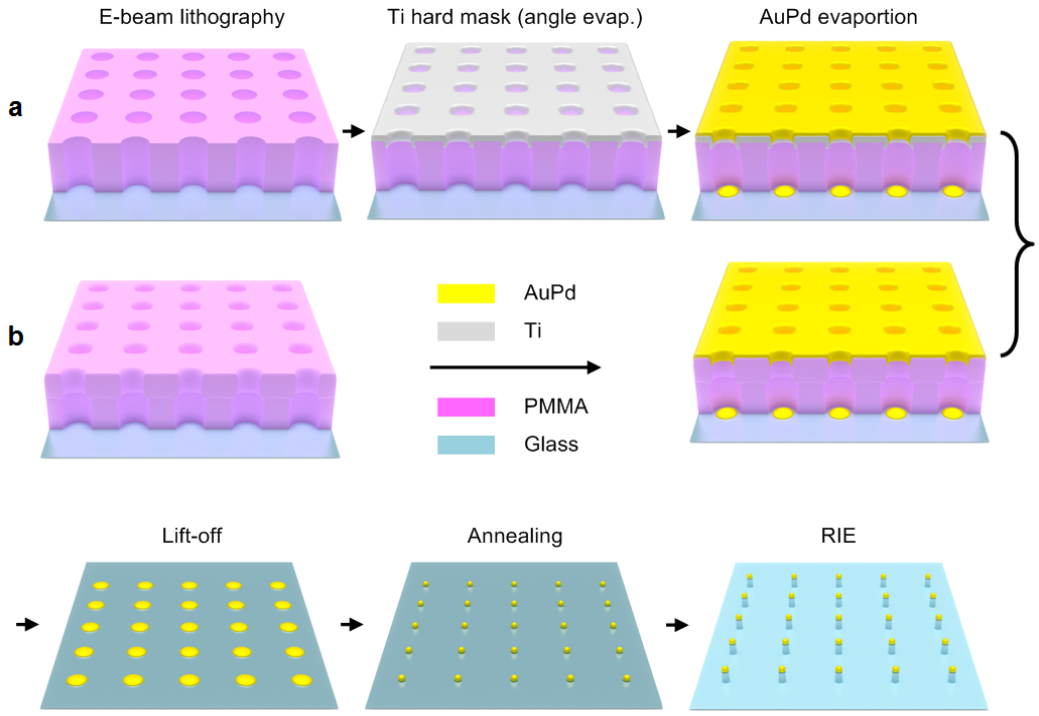

Supplementary Figure S1. **Nanoarray fabrication processes flow.** Either (a) single resist layer with hard mask, or (b) resist bilayer was used to facilitate the lift-off process. (a) Electron beam exposure and resist development are followed by angle deposition of a thin (~ 10 nm) film of Ti, which coats the top surface of the resist and the upper edges of the sidewalls of the patterned openings. A short oxygen plasma etches resist residue and broadens the resist openings under the Ti, facilitating easy lift-off of the AuPd (~ 1 – 3 nm) that is deposited by electron beam evaporation. (b) An undercut profile of the resist is achieved by using a bilayer resist consisting of two different Mw layers of PMMA. AuPd deposition and lift-off are similar to (a). Bottom panel shows schematically how the AuPd platelets remaining after lift-off are transformed to nanoparticles by thermal annealing. Reactive ion etching of the glass forms 10 nm pedestal beneath the nanoparticles. Process details are included in Methods.

Nanoarray geometries

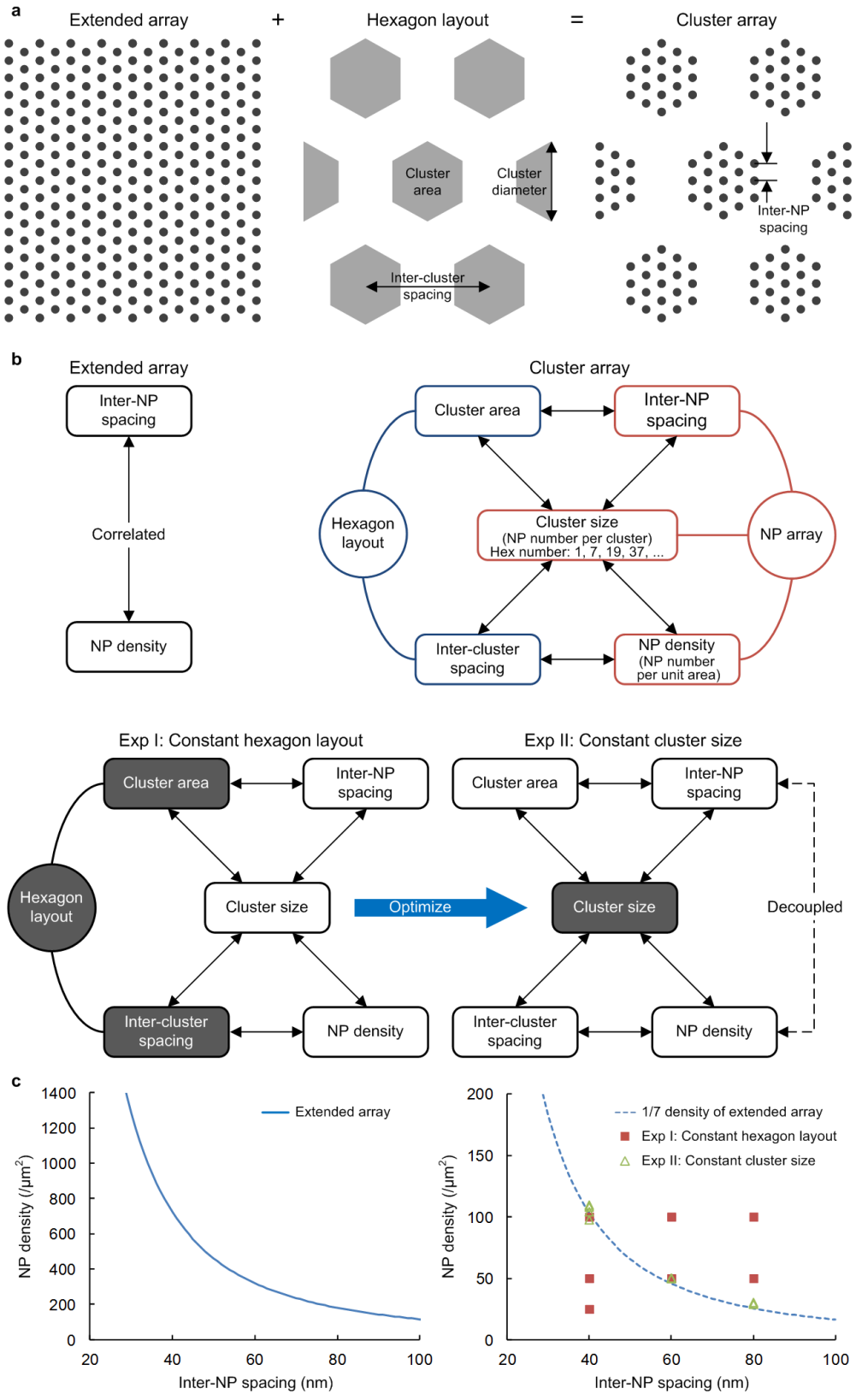

Supplementary Figure S2. Systemicatic variation of **NP array geometric parameters to probe effects on T cell activation.** (a) Schematics of extended and cluster arrays. For the sake of isotropy and symmetry, a hexagon layout is applied to generate cluster arrays from the extended hexagonal arrays. For cluster arrays, the NP geometric arragements maintain that of extended arrays in each hexgon island, while acheving a lower global NP density. (b) Geometric parameters and their relations. For extended arrays, there are only two correlated parameters of inter-NP spacing and NP density. For cluster arrays, there is one more parameter of cluster size (NP number per cluster), which is always a centered hexagonal number by filling a hexagon island with extended arrays. There are also hexagon layout parameters including cluster area and inter-cluster spacing, related with the NP array parameters. Given the complexity, two steps were carried out to vary the parameters systematically. In Exp I, hexagon layouts were kept constant for various NP array parameters, and were optimized to obtain pY singnaling comparable to extended arrays but at a much lower (~1/7) NP density. In Exp II, the optimized cluster size were kept constant, in order to further decouple and compare the indepednt effects of inter-NP spacing and NP density. (c) The relation between two major geometric parameters, inter-NP spacing and NP density, for extended and cluster arrays. In Exp I, the cluster arry density is ~1/7 of extended array, but the two parameters are still correlated. In Exp II, the two parameters are completely decoupled and more combinations are explored.

Note

Nanoarray patterns are named by the following convention:

Extended hexagonal arrays: “h” + “inter-NP spacing value” (nm) + “d” + NP density value” (/μm^2).

Cluster arrays: “c” + “NP per cluster value” + “s” + “inter-NP spacing value” (nm) + “d” + “NP density value” (/μm^2).

For example, "c127s40d50" represents a cluster array with 127 NPs per cluster, 40 nm inter-NP spacing and 50 /μm^2 global density.

NP functionalization scheme

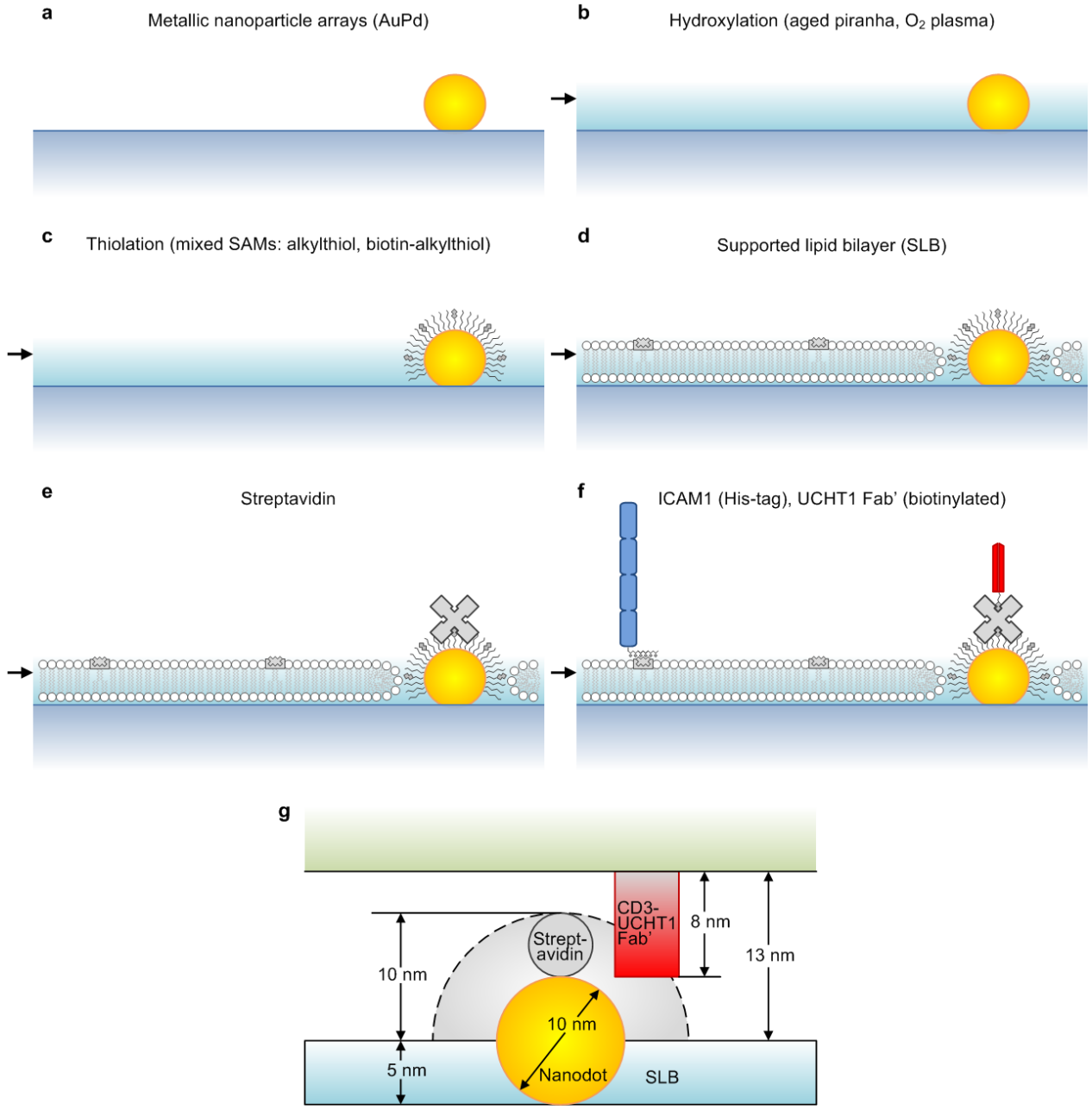

Supplementary Figure S3. **Functionalization scheme and formation of supported lipid bilayer (SLB).** Starting with the patterned AuPd NPs on the glass surface (a), hydroxyl groups are formed on using aged piranha and oxygen plasma (b). Mixed self-assembled monolayers of alkylthiols and biotinylated alkylthiols are formed on the NPs (c), followed by formation of the DGS-NTA(Ni)-loaded SLB on the surrounding glass surface (d). A streptavidin bridge binds to the biotins on the NPs (e) to facilitate the binding of Alexa 568-UCHT1 Fab' to the NPs. Alexa 405-ICAM1 binds to the SLB via a His-tag linker (f). (g) Estimation of the spacing between SLB and engaged T cell.

Streptavidin (PDB: 1MK5) is 4.2×4.9×5.4 nm^3, and approximated by a sphere with diameter ~ 5 nm. The maximum total height of NP and streptavidin above SLB is ~ 10 nm, but UCHT1 Fab' could be binding anywhere on the hemisphere (blue region), so it is estimated as ~ 5 nm above the SLB on average. CD3-UCHT1 Fab' complex (PDB: 1XIW) is 4.9×6.1×8 nm^3, so the axial size is ~ 8 nm. Therefore, the intermembrane spacing is estimated as ~ 13 nm, which is similar to the TCR-pMHC junction between T cell and APC (Fig. 1a); recent studies demonstrate that this spacing is adequate to significantly excluded CD45 based on the inter-membrane separation only[1]. Thus, the rigid 10 nm pedestals should increase the intermembrane separation to 23 nm. This is predicted to allow CD45 access to the TCR cluster on the 3D, but not 2D arrays[2].

UCHT1 Fab' intensity on nanoarrays

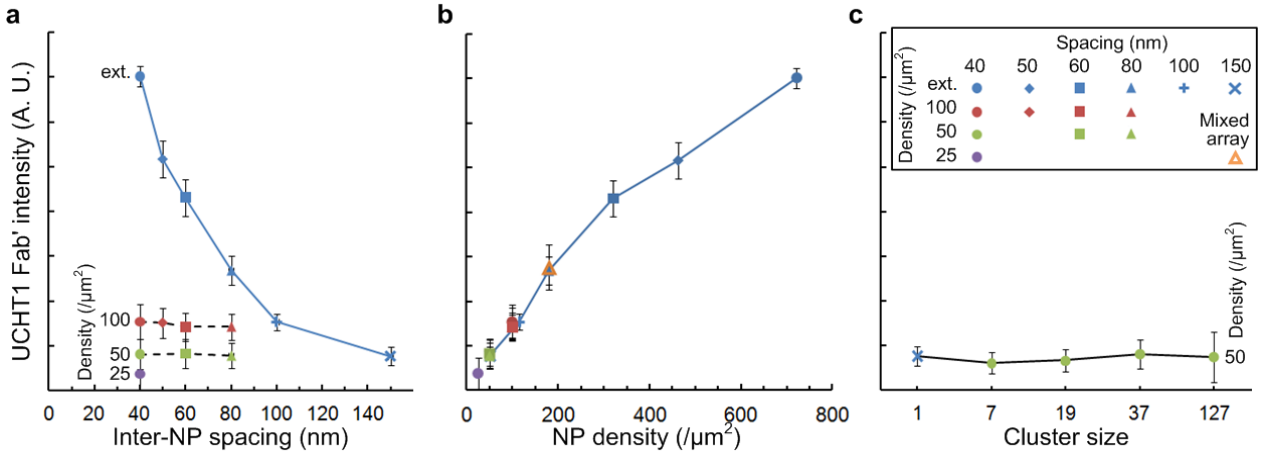

Supplementary Figure S4. **UCHT1 Fab' intensity on nanoarrays with various geometries.** Plots against (a) inter-NP spacing, (b) NP density, (c) cluster size. Data are means ± s.d., n = 5 locations on 200 × 200 μm^2 nanoarrays. Nanoarray geometries from Exp II (refer to Supplementary Fig. S9, 10g for details).

This indicates that the NPs penetrate the SLB, rather than being covered by it. Moreover, the Fab' intensity scaled linearly with NP density, which suggests that the NPs were closely surrounded by the SLB with no significant edge effects (defective coverage around NPs), consistent with earlier work[3, 4, 5], and the sidewalls of the pedestals did not increase non-specific binding, as they were likely covered with lipid membrane and/or blocked by casein. This is important because defects in the SLB, especially around the NPs, would result in nonspecific adsorption of UCHT1 Fab' and could alter cellular response.

UCHT1 Fab' molecular occupancy

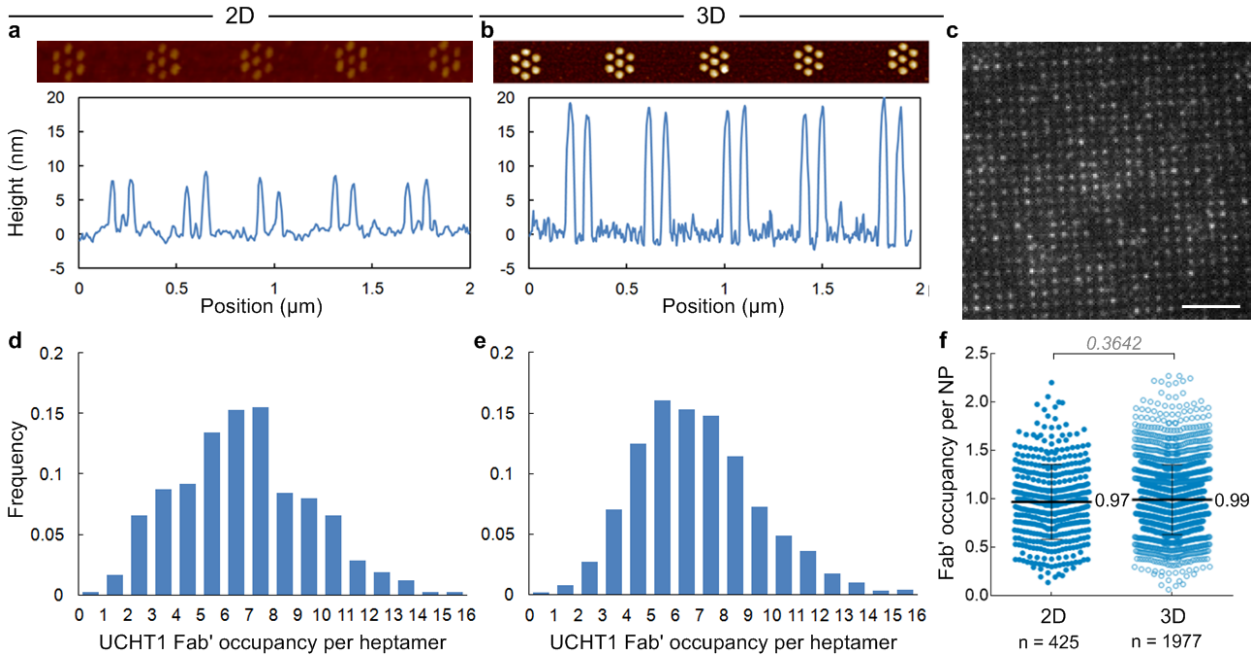

Supplementary Figure S5. **UCHT1 Fab' molecular occupancy analysis by a bleaching technique: 2D vs. 3D surfaces.** (a) 2D and (b) 3D NP heptamers (c7s40d7) provide higher signal-to-background ratio than single NPs. (c) Typical fluorescence image of 1µm-spaced heptamers (c7s40d7), scale bar 5 µm. The experiment was repeated 10 times independently with similar results. Histograms of UCHT1 Fab' occupancy per heptamer on (e) 2D and (f) 3D surfaces. (f) Fab' occupancy per NP ~ 1, with 80% of single NPs having at least 1 UCHT1-Fab' (which is better than the Poisson distribution)[6], without significant difference between 2D and 3D surfaces. Data are means ± s.d., each point representing the Fab' occupancy measured on a heptamer, n > 425 measurements (Mann–Whitney test, two-sided).

SLB mobility on nanoarrays

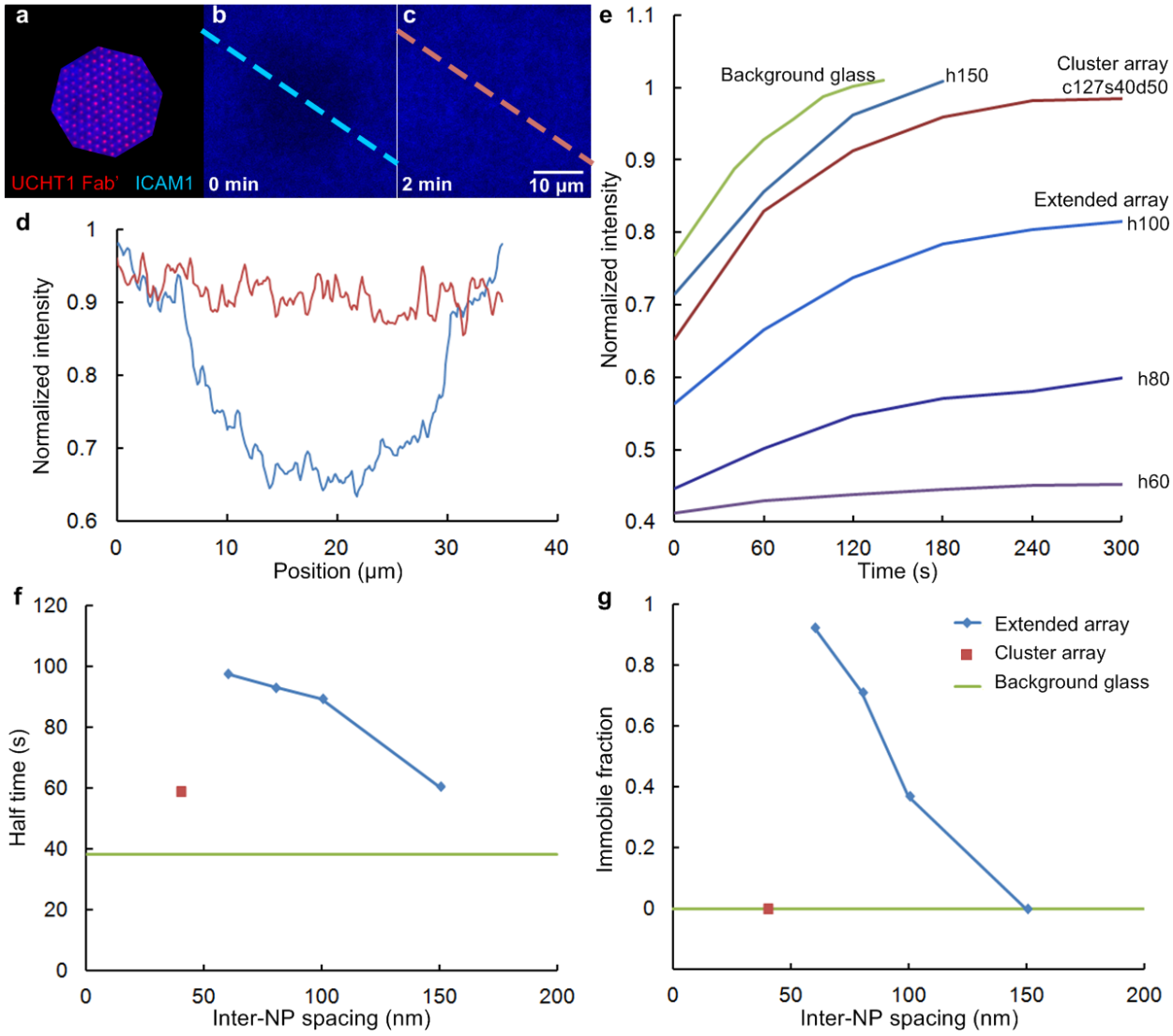

Supplementary Figure S6. **FRAP shows SLB continuity and mobility.** (a) The fluorescence image of UCHT1 Fab' and ICAM1 on a cluster array c127s40d50. (b) A bleached central spot in the SLB. (c) Fluorescence recovery after 2 min. (d) Line scans of the FRAP. The dependence of ICAM1 mobility on the NP array geometry: (e) Recovery curves of SLB on various NP arrays. (f) Half time of recovery and (g) immobile fraction vs. inter-NP spacing. For direct comparison, the data are from various nanoarrays on the same surface backfilled with SLB. The experiment was repeated 3 times independently with similar results.

pY vs. pZAP70 as an indicator of TCR triggering in Exp. I

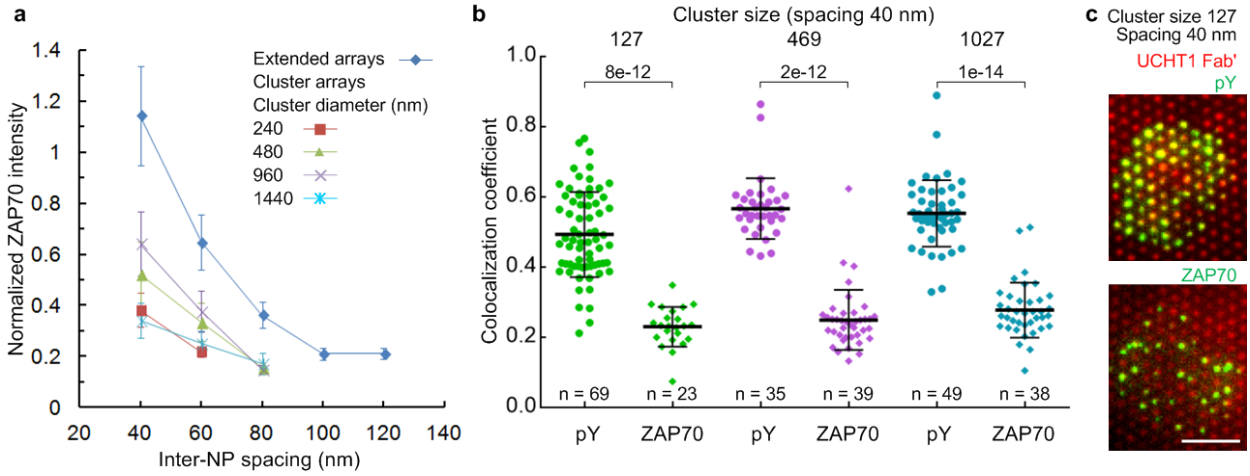

Supplementary Figure S7. **pZAP70 as an indicator of T cell signaling on 2D surfaces.** (a) Normalized pZAP70 intensity vs. inter-NP spacing. Compared with pY signal in Fig. 2b, pZAP70 shows a similar spacing effect, but the signal is much lower with larger uncertainty (standard deviation). Data are means ± s.e.m, n > 30 cells from 2 independent experiments. (b) Mander's correlation coefficient (M1, percentage of total signal from UCHT1 Fab' which overlaps with T cell signaling) of clusters with different cluster sizes (inter-NP spacing 40 nm). The colocaliation of pY is significantly higher than that of pZAP70. Data are means ± s.d., each point representing a cell, n > 23 cells from 2 independent experiments (Mann–Whitney test, two-sided). (c) Representative fluorescence images of pY and ZAP70 (c127s40d104, size bar = 5 µm). Nanoarray geometries from Exp I (refer to Fig. 2a for details). The experiment with pY was repeated 3 times independently with similar results. The experiment with ZAP70 was repeated 2 times independently with similar results.

The relatively weaker signal of pZAP70 and its lower degree of colocalization are likely due to the fact that the TCR proximal kinases phosphorylate many substrates including LAT, PLCG1 and HCLS1, which are all associated generating robust calcium signals. This is now fairly well understood (see, e.g., Mossman et al.[7], where pY is used as a readout for signaling in TCR micro clusters induced by patterned SLBs and this signal did predict other T cell responses in that context.

pY colocalization and T cell spreading in Exp. I

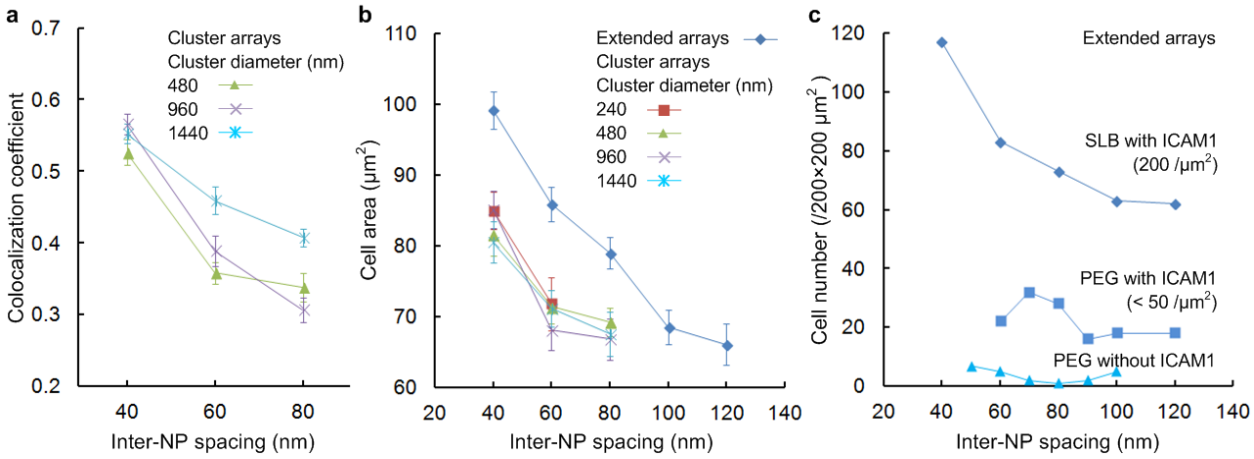

Supplementary Figure S8. **Spacing effect on pY colocalization and cell adhesion/spreading.** (a) Mander's colocalization coefficient[8] for pY on UCHT1 Fab'. Data are means ± s.e.m., n > 25 cells from 2 independent experiments. (b) Cell spreading area. Data are means ± s.e.m., n > 48 cells from 3 independent experiments, as summarized in Supplementary Table S1. (c) Number of cells adhered on 200 × 200 μm^2 extended arrays. SLB with mobile ICAM1 provides better adhesion than PEG (polyethylene glycol) passivation. Nanoarray geometries from Exp I (refer to Fig. 2a for details).

Statistical details of data from Exp. I (Fig. 2)

Supplementary Table S1. **Precise sample size n and p-values (Mann–Whitney test, two-sided) of Exp. I (Fig. 2)**. Each row corresponds to the nanoarray geometry (cluster arrays sorted by the cluster diameter), and each column corresponds to the inter-NP spacing, the same as in Fig. 2a. Each table cell contains the pattern name and sample size n (i.e., number of T cells used in measurements). Lines between two table cells indicate the p-values between two patterns. The difference is not significant if p-value > 0.05 (italic).

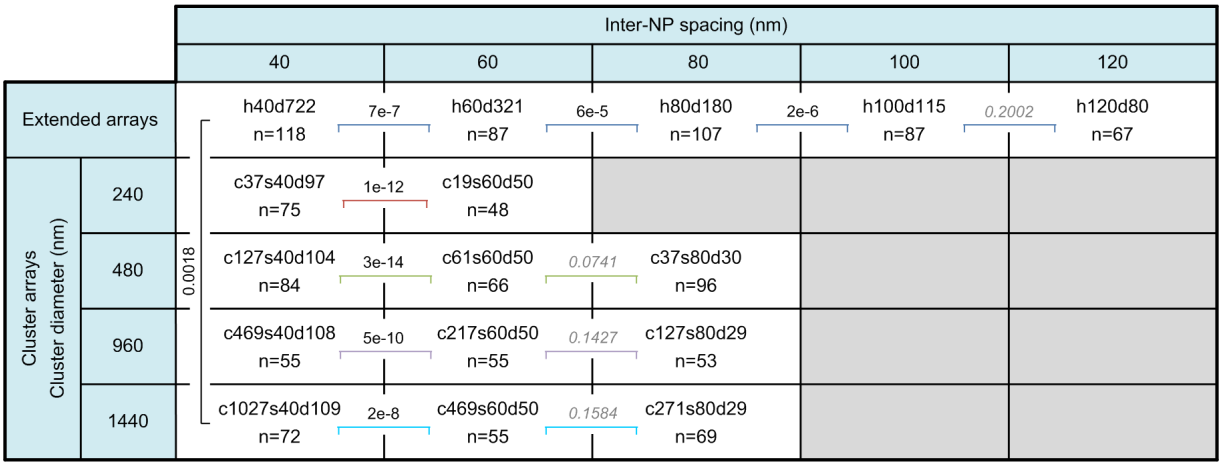

Nanoarray cluster geometries used in Exp. II (Fig. 3)

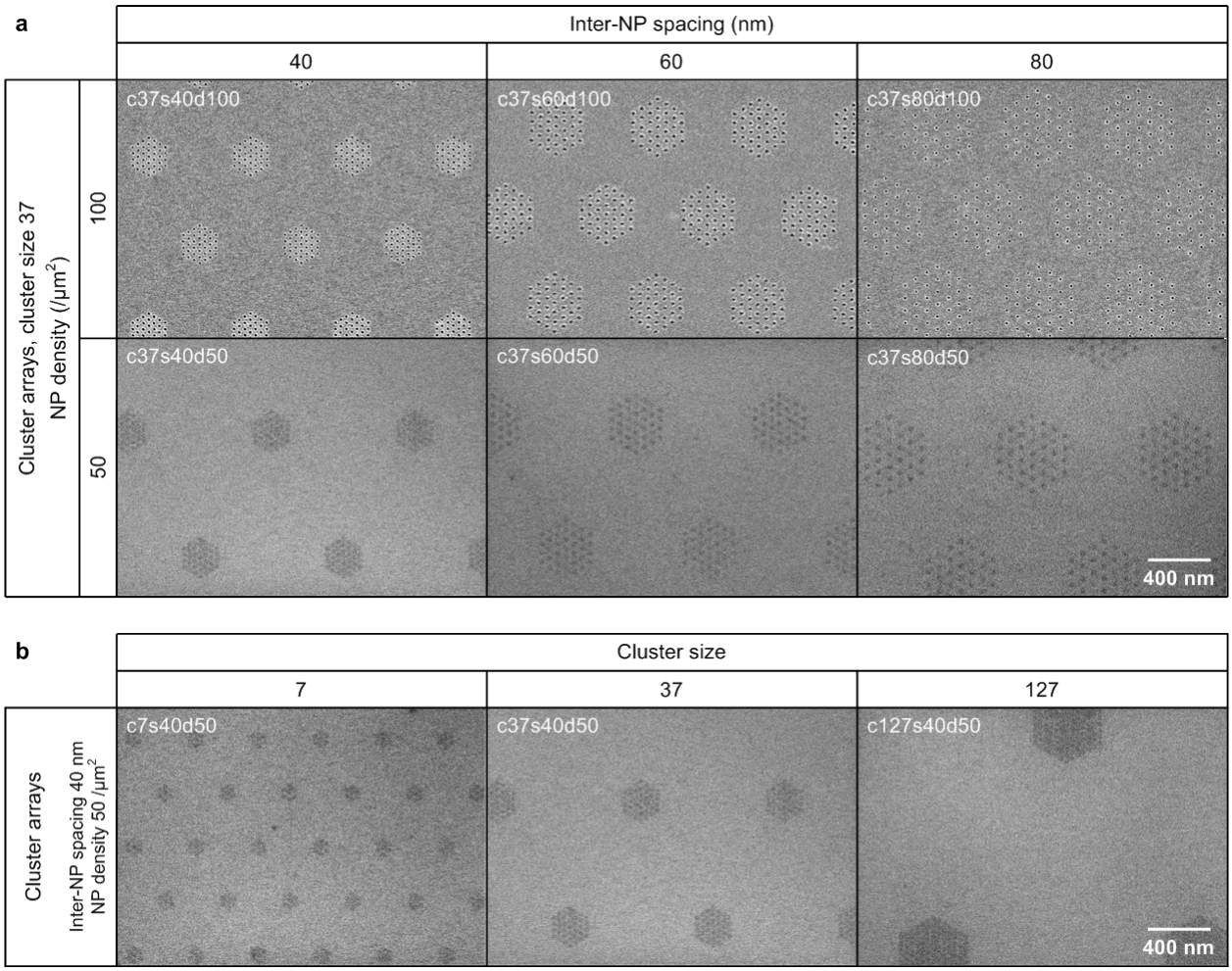

Supplementary Figure S9. **Nanoarray geometries from Exp II**. SEM images of cluster arrays (AuPd, before or after lift-off): (a) Arrays with the optimized cluster size of 37 NPs, and decoupled inter-NP spacing and NP density. (b) Arrays with 40 nm inter-NP spacing, 50 NP/μm^2 density, and various cluster size.

Detailed plots of data from Exp. II (Fig. 3)

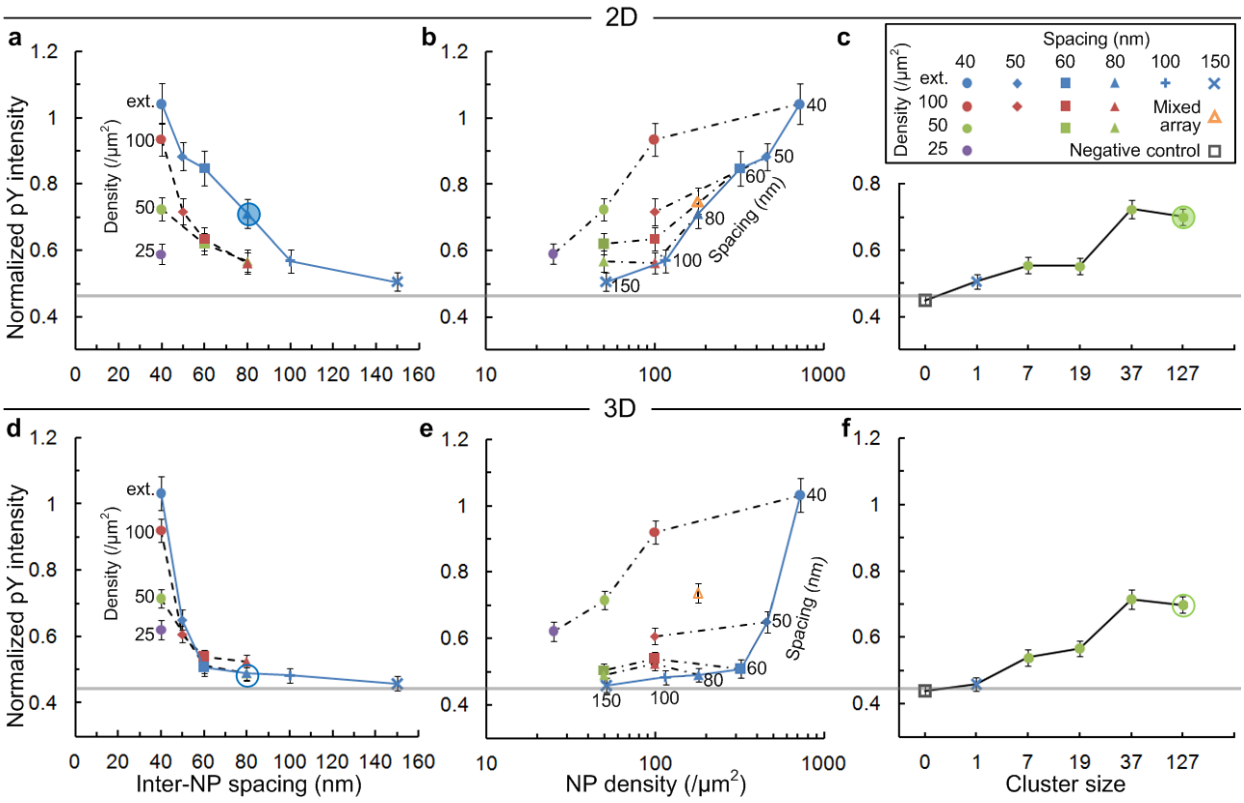

Supplementary Figure S10. **Replots of Exp II data in Fig. 3, 4, with detailed symbols indicating the array geometry corresponding to each data point.** Data are means ± s.e.m., n > 180 cells from 3 independent experiments. Statistical details and symbols annotations are summarized in Supplementary Table S2.

Statistical details of data from Exp. II (Fig. 3)

Supplementary Table S2. **Precise sample size n and p-values (Mann–Whitney test, two-sided) of Exp. II (Fig. 3) and symbol annotations of Fig. S10.** Each row corresponds to the nanoarray geometry (cluster arrays sorted by the NP density), and each column corresponds to the inter-NP spacing or cluster size. Each table cell contains the pattern name and sample size n (i.e., number of T cells used in measurements). Lines between two table cells indicate the p-values between two patterns. The difference is not significant if p-value > 0.05 (italic).

2D

		Inter-NP spacing s (nm)					
		40	50	60	80	100	150
Extended arrays		h40d722 ● n=218	h50d462 ◆ n=196	h60d321 ■ n=209	h80d180 ▲ n=190	h100d115 + n=200	h150d51 × n=191
Cluster arrays, c=37 NP density d (/μm²)	100	c37s40d100 ● n=237	c37s50d100 ◆ n=189	c37s60d100 ■ n=224	c37s80d100 ▲ n=216		
	50	c37s40d50 ● n=209		c37s60d50 ■ n=197	c37s80d50 ▲ n=221		
	25	c37s40d25 ● n=223					

p-values: 0.0069 (h80d180 – h100d115); *0.4277* (h100d115 – h150d51); 1e-5 (c37s40d100 – c37s50d100); *0.1366* (c37s60d100 – c37s80d100); 0.0329 (c37s40d100 – c37s40d50); *0.0942* (c37s60d50 – c37s80d50)

		Cluster size c				Mixed arrays	Negative control
		7	19	37	127		
Cluster arrays s = 40 nm d = 50 /μm²		c7s40d50 ● n=192	c19s40d50 ● n=215	c37s40d50 ● n=209	c127s40d50 ● n=206	c127s40d50/h80d180 △ n=196	Glass background □ n=335

p-values: *0.8178* (c7s40d50 – c19s40d50); 0.0001 (c19s40d50 – c37s40d50)

3D

		Inter-NP spacing s (nm)					
		40	50	60	80	100	150
Extended arrays		h40d722 ● n=333	h50d462 ◆ n=264	h60d321 ■ n=251	h80d180 ▲ n=293	h100d115 + n=254	h150d51 × n=282
Cluster arrays, c=37 NP density d (/μm²)	100	c37s40d100 ● n=276	c37s50d100 ◆ n=307	c37s60d100 ■ n=371	c37s80d100 ▲ n=336		
	50	c37s40d50 ● n=317		c37s60d50 ■ n=263	c37s80d50 ▲ n=266		
	25	c37s40d25 ● n=303					

p-values: 6e-5 (h50d462 – h60d321); *0.1463* (h60d321 – h80d180); 1e-20 (c37s40d100 – c37s50d100); *0.7372* (c37s60d100 – c37s80d100); 2e-8 (c37s40d100 – c37s40d50); *0.2356* (c37s60d50 – c37s80d50)

		Cluster size c				Mixed arrays	Negative control
		7	19	37	127		
Cluster arrays s = 40 nm d = 50 /μm²		c7s40d50 ● n=306	c19s40d50 ● n=292	c37s40d50 ● n=317	c127s40d50 ● n=317	c127s40d50/h80d180 △ n=346	Glass background □ n=481

p-values: *0.2714* (c7s40d50 – c19s40d50); 7e-6 (c19s40d50 – c37s40d50)

TCR triggering and T cell spreading on small clusters

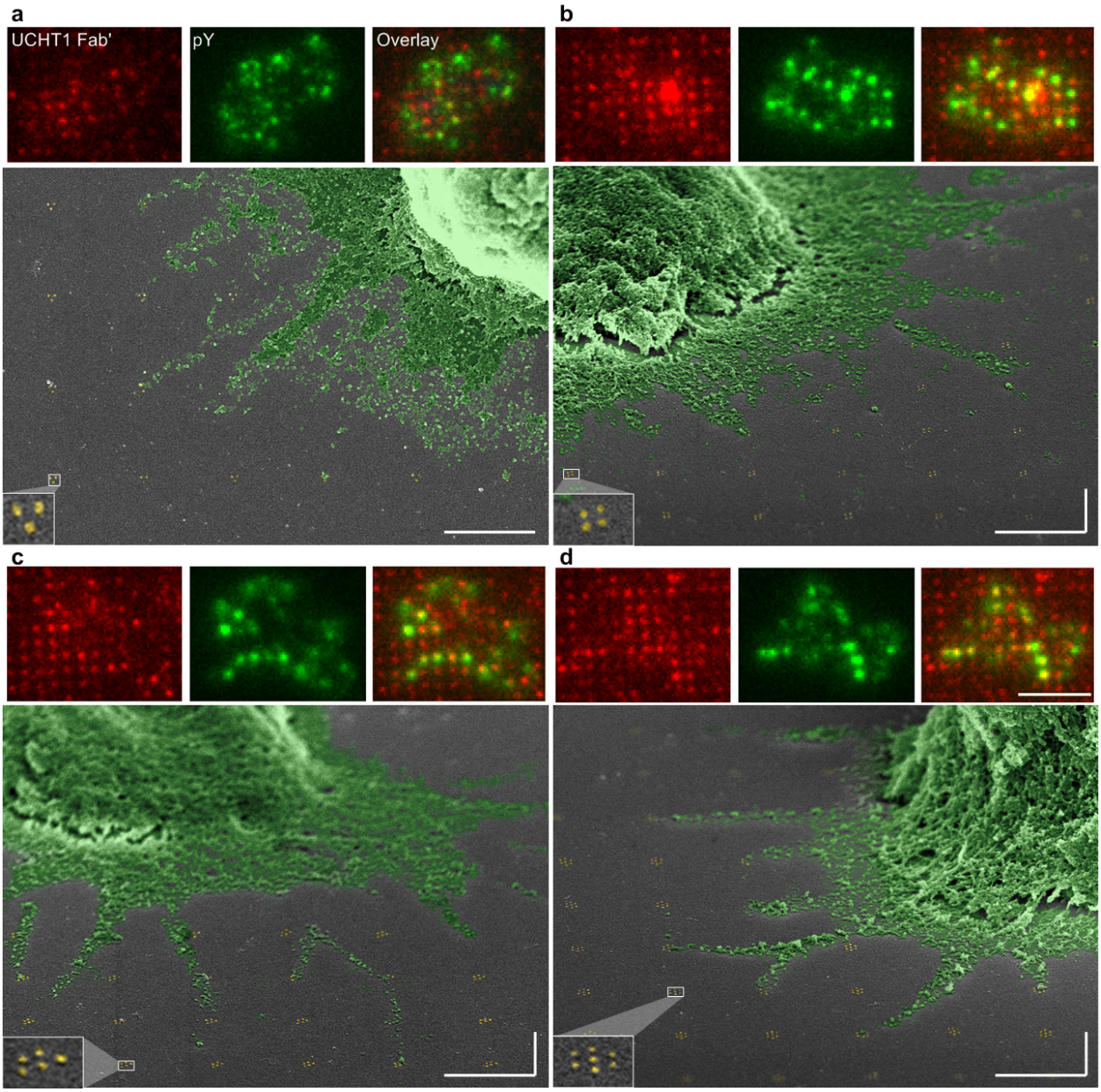

Supplementary Figure S11. **Local TCR triggering on small clusters on 2D surfaces.** Cluster sizes are (a) 3, (b) 4, (c) 5, (d) 7 NPs. Fluorescence images indicate the pY signaling colocalized with UCHT1 Fab'. SEM images show filopodia contacting individual clusters. Pseudo-color, size bar = 1 μm. Inset shows zoom-in of a NP cluster in focus. The fluorescence imaging was repeated 6 times independently with similar results. The SEM imaging was repeated 2 times independently with similar results.

CD45 exclusion on clusters

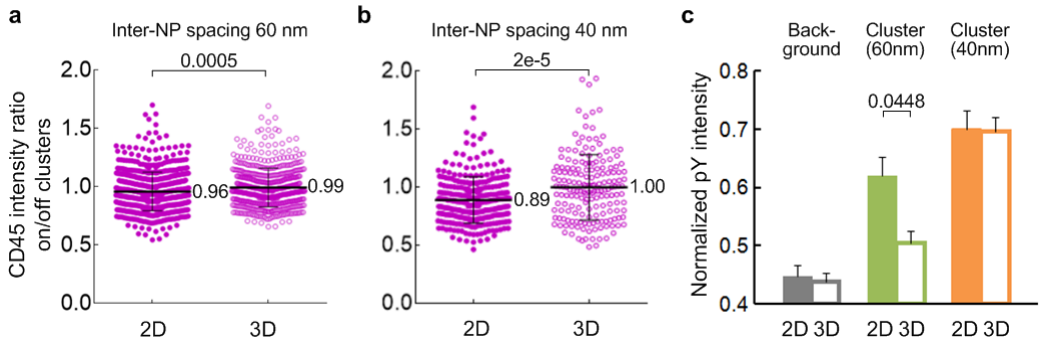

Supplementary Figure S12. **CD45 exclusion on clusters: 2D vs. 3D surfaces.** (a) Inter-NP spacing 60 nm (c37s60d50), (b) inter-NP spacing 40 nm (c127s40d50, data from Fig. 6c). Data are means ± s.d., each point representing a cluster in cell, n = 8 cells from 2 independent experiments for each data set (Mann–Whitney test, two-sided). Note that the absolute values are not directly comparable between 60nm and 40nm on 2D surfaces, because the cluster hexagon layouts are different. (c) Normalized pY intensity (data from Fig. 3). Data are means ± s.e.m., n > 180 cells from 3 independent experiments (Mann–Whitney test, two-sided). The exact sample sizes are summarized in Supplementary Table S2. The pY signal is lower on 3D than 2D on 60 nm clusters, probably due to the weaker CD45 exclusion, in agreement with the KS model. On the other hand, the pY signal is maintained on 40 nm clusters, despite weaker CD45 exclusion.

TCR packing model

While antibody and soluble pMHC dimers both can trigger T cells through cross-linking[9, 10], the lateral spacing threshold we observe for clustering on the 3D substrates is ~ 10 times larger. The ability to trigger signals at 10-fold lower effective engaged TCR density may reflect the contribution of LFA1 outside-in signaling to TCR triggering, which includes promotion of ZAP70 activation[11]. Regardless, surface stimulation seems to operate with greater inter-molecular spacing than crosslinking by soluble antibodies or pMHC dimers. On the other hand, full T cell activation by an antigen presenting cell can involve as few as 10 pMHC spread over a 50 μm^2 contact area[12]. The density and cluster size requirements reported here for a whole cell response are less sensitive (a density > 25 NP/μm^2, and a cluster size > 19 NP); this may be due in part to the inability of the Fab' to engage the CD4 co-receptor, which is in part responsible for the ultrasensitivity of TCR to pMHC[12]. While we were able to optimally stimulate T cells with cluster arrays with an average density of ~100 /μm^2, the local density at 40 nm inter-NP spacing is 722 /μm^2, which seems very high. This is, however, consistent with the case of T cells interacting with TCR clusters with a density of ~1500 /μm^2 on anti-CD3 coated surfaces[13]. This level of clustering may be facilitated by the high affinity of antibodies like UCHT1 for the TCR complex. Further study is needed to determine whether lower affinity antibodies and pMHC interactions will also operate with a similar spacing threshold when the intermembrane distance is increased[14].

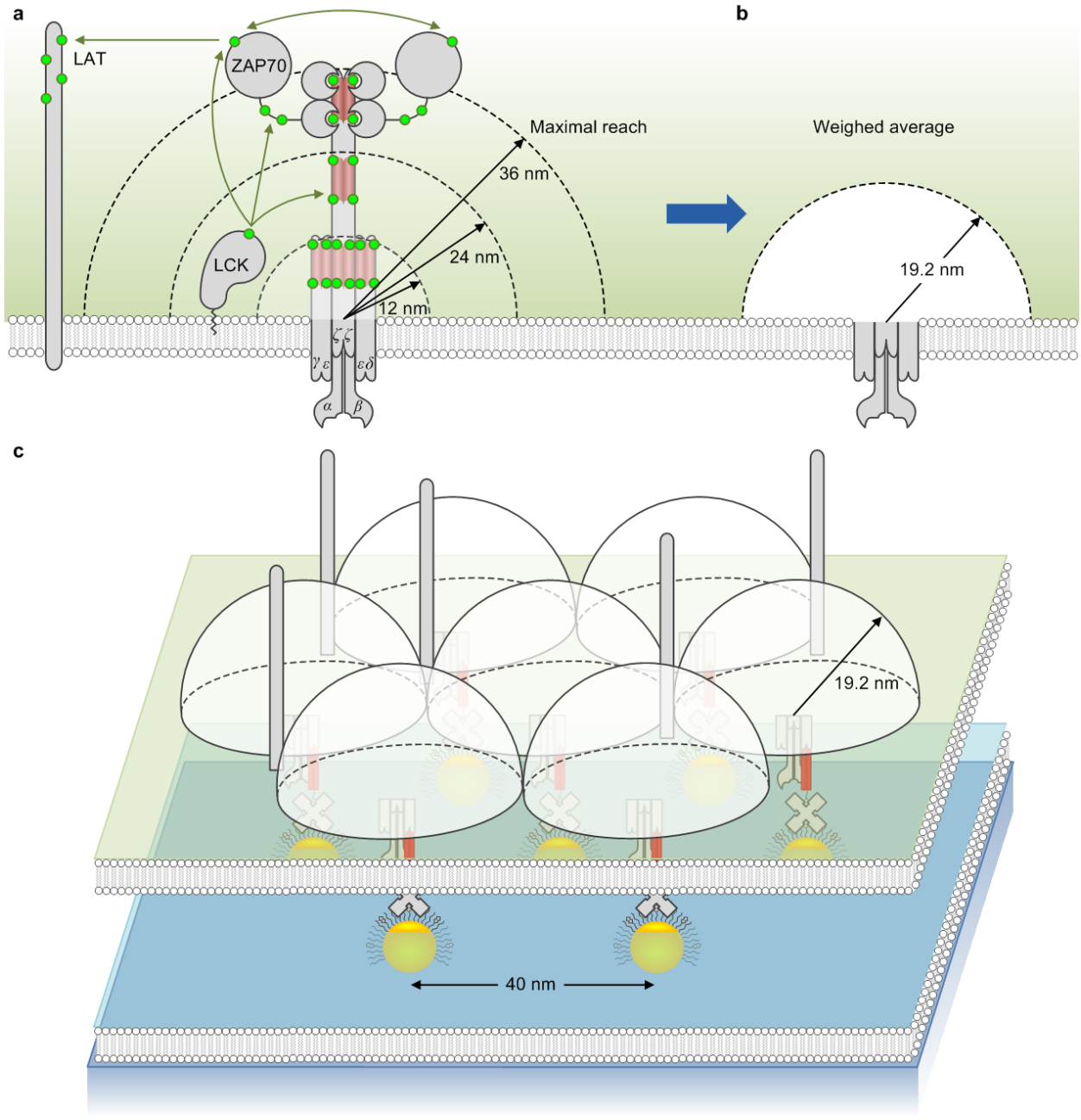

Supplementary Figure S13. **Model for TCR packing in clusters with <50 nm spacing.** Schematics of TCR cytoplasmic domains and a small TCR microcluster triggered by a nanopattern. (a) The maximal reach and (b) weighted average of the cytoplasmic ITAMs and associated kinase ZAP70. (c) TCR packing at the level of the cytoplasmic domains may be achieved only at a 40 nm spacing required for triggering when CD45 cannot be excluded due to close inter-membrane separation.

ICAM1 exclusion

In addition to segregation of CD45, discussed in the main text, we also observed selective exclusion of ICAM1, which is similar in size to CD45[15], from the UCHT1 Fab' clusters on 2D surfaces (Supplementary Fig. 15). ICAM1 was also absent from a larger central regions 2-3 μm across on 2D substrates, indicative of central F-actin clearing and secretory domain formation in immunological synapses[16] (Supplementary Fig. 15a-c). Interestingly, the central clearing of ICAM1 was not observed on the 3D surfaces (Supplementary Fig. 15d). This suggests that the 2D surfaces generate a central secretory domain, whereas the 3D surfaces do not. This implies that failure to effectively exclude CD45 and other effects of the 3D substrates on TCR signaling may be compensated for by close UCHT1 Fab' spacing, but qualitative differences in resulting synapses may have an impact on other functions such as directed secretion. This requires further investigation.

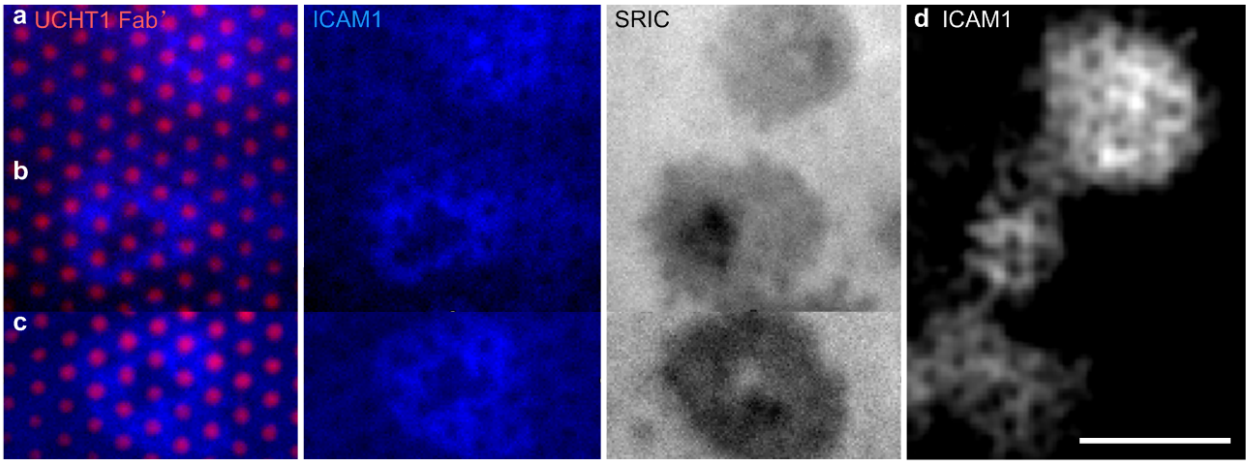

Supplementary Figure S14. **ICAM1 distribution of T cells: 2D vs. 3D surfaces.** 2D surfaces: (a) central region is not depleted; (b) central region is depleted for most cells; (c) central region is depleted and the cell forms a void above the surface, consistent with the micro-vesicle model. 3D surfaces: (d) central region is not depleted. Size bar = 10 μm. The SEM imaging was repeated 3 times independently with similar results.

ROI selection

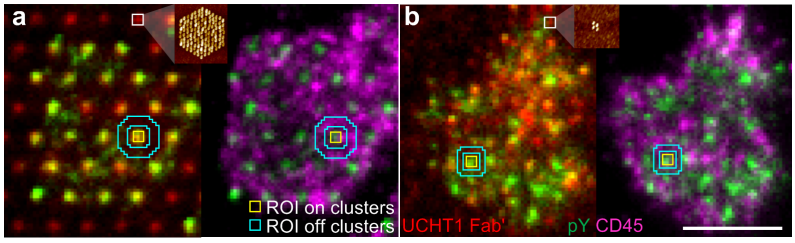

Supplementary Figure S15. **ROI selection for the quantification of intensity ratio on/off clusters.** (a) Large clusters (cluster size 127, density 50 /μm^2). (b) Small clusters (cluster size 4, density 4 /μm^2). Size bar = 5 μm**.**

References

1. Carbone, C B, Kern, N, Fernandes, R A, Hui, E F, Su, X L*, et al.* In vitro reconstitution of T cell receptor-mediated segregation of the CD45 phosphatase. *Proceedings of the National Academy of Sciences of the United States of America* 2017, **114**(44)**:** E9338-E9345.

2. Chang, V T, Fernandes, R A, Ganzinger, K A, Lee, S F, Siebold, C*, et al.* Initiation of T cell signaling by CD45 segregation at 'close contacts'. *Nat Immunol* 2016, **17**(5)**:** 574-582.

3. Lohmuller, T, Triffo, S, O'Donoghue, G P, Xu, Q, Coyle, M P*, et al.* Supported membranes embedded with fixed arrays of gold nanoparticles. *Nano Lett* 2011, **11**(11)**:** 4912-4918.

4. Roiter, Y, Ornatska, M, Rammohan, A R, Balakrishnan, J, Heine, D R*, et al.* Interaction of Nanoparticles with Lipid Membrane. *Nano Letters* 2008, **8**(3)**:** 941-944.

5. Roiter, Y, Ornatska, M, Rammohan, A R, Balakrishnan, J, Heine, D R*, et al.* Interaction of Lipid Membrane with Nanostructured Surfaces. *Langmuir* 2009, **25**(11)**:** 6287-6299.

6. Cai, H, Wolfenson, H, Depoil, D, Dustin, M L, Sheetz, M P*, et al.* Molecular Occupancy of Nanodot Arrays. *ACS Nano* 2016.

7. Mossman, K D, Campi, G, Groves, J T, Dustin, M L. Altered TCR signaling from geometrically repatterned immunological synapses. *Science* 2005, **310**(5751)**:** 1191-1193.

8. Dunn, K W, Kamocka, M M, McDonald, J H. A practical guide to evaluating colocalization in biological microscopy. *American Journal of Physiology-Cell Physiology* 2011, **300**(4)**:** C723-C742.

9. Cochran, J R, Cameron, T O, Stern, L J. The relationship of MHC-peptide binding and T cell activation probed using chemically defined MHC class II oligomers. *Immunity* 2000, **12**(3)**:** 241-250.

10. Cochran, J R, Cameron, T O, Stone, J D, Lubetsky, J B, Stern, L J. Receptor proximity, not intermolecular orientation, is critical for triggering T-cell activation. *J Biol Chem* 2001, **276**(30)**:** 28068-28074.

11. Evans, R, Lellouch, A C, Svensson, L, McDowall, A, Hogg, N. The integrin LFA-1 signals through ZAP-70 to regulate expression of high-affinity LFA-1 on T lymphocytes. *Blood* 2011, **117**(12)**:** 3331.

12. Irvine, D J, Purbhoo, M A, Krogsgaard, M, Davis, M M. Direct observation of ligand recognition by T cells. *Nature* 2002, **419**(6909)**:** 845-849.

13. Sherman, E, Barr, V, Manley, S, Patterson, G, Balagopalan, L*, et al.* Functional Nanoscale Organization of Signaling Molecules Downstream of the T Cell Antigen Receptor. *Immunity* 2011, **35**(5)**:** 705-720.

14. Chen, B M, Al-Aghbar, M A, Lee, C H, Chang, T C, Su, Y C*, et al.* The Affinity of Elongated Membrane-Tethered Ligands Determines Potency of T Cell Receptor Triggering. *Front Immunol* 2017, **8:** 793.

15. Yang, Y, Jun, C D, Liu, J H, Zhang, R, Joachimiak, A*, et al.* Structural basis for dimerization of ICAM-1 on the cell surface. *Mol Cell* 2004, **14**(2)**:** 269-276.

16. Ritter, Alex T, Asano, Y, Stinchcombe, Jane C, Dieckmann, N M G, Chen, B-C*, et al.* Actin Depletion Initiates Events Leading to Granule Secretion at the Immunological Synapse. *Immunity* 2015, **42**(5)**:** 864-876.